THE BELL SYSTEM TECHNICAL JOURNAL
Vol. 55, No. 1, January 1976
Printed in U.S.A.

The Jitter Performance of Phase-Locked Loops Extracting Timing From Baseband Data Waveforms

By D. L. DUTTWEILER

(Manuscript received June 3, 1975)

Phase comparators used in phase-locked loops extracting symbol timing from baseband data waveforms typically only produce a useful error signal when a data transition occurs. This gating of the error signal by data transitions makes the natural model for studying jitter in such phase-locked loops time-varying and difficult to analyze. In this paper we show how, under good approximation, it can be simplified to a time-invariant model that is easily analyzed. Using this model, we study jitter accumulation along chains of digital repeaters with phase-locked-loop timing extractors. A numerical example is given.

I. INTRODUCTION

To decode a baseband data waveform, a clock signal giving the proper sampling time must be available. Pilot tones are sometimes transmitted along with the data waveform for this purpose but, alternately, timing can be derived directly from the data waveform itself. One approach to self-timing is to let the data waveform passed through a memoryless nonlinearity ring a tuned circuit with a resonant frequency close to the nominal signaling rate.[1–8] Another technique, which in general involves more circuitry but gives superior performance, is to use a phase-locked loop (PLL).

The element of a PLL extracting symbol timing that is most interesting functionally is its phase comparator. Numerous realizations are possible. Almost all these realizations are similar, however, in that they only produce an error signal when a data transition occurs. The gating of the error signal by data transitions in a PLL extracting symbol timing makes the analysis of such a PLL potentially quite different from the analysis of phase-locked loops used in other applications.

For purposes such as studying timing acquisition, the effect of transition gating is adequately modeled as a multiplication of the

phase comparator gain in the presence of a data transition by the probability p of a data transition. After this approximation is made, the loop has the conventional structure. For studying jitter, however, this model is not satisfactory because transition gating is itself often an important source of jitter that of necessity is neglected when the average-gain approximation is made. As will be discussed more fully later, transition gating produces jitter by chopping the static phase error needed to pull the voltage-controlled oscillator (VCO) from its natural frequency to the line frequency and thereby injecting wideband noise into the loop.

The purpose of this paper is to develop a time-invariant linear model for a PLL with transition gating that adequately mirrors, even for jitter-studying purposes, the effects of transition gating. The model we obtain differs from the linear model obtained by simply making the average-gain approximation in the addition of an additive wideband noise representative of the chopping of the static phase error by transition gating.

With the time-invariant linear model available, it is straightforward to calculate the spectrum and variance of the jitter on the output of a PLL extracting symbol timing from a data waveform. We conclude with a discussion of jitter accumulation along chains of digital repeaters with PLL timing extractors.

Saltzberg[9] and Roza[10] have both previously done excellent work analyzing phase-locked loops extracting symbol timing. Our work is closer to Saltzberg's, and we use many of his results. Saltzberg was able to obtain equations for the jitter spectrum and jitter variance directly from the natural gated model. The equations we obtain from the approximate model are similar, but they are obtained with much less difficulty and without needing to assume one-sided intersymbol interference.

Roza's analysis is at a more abstract level. His equations for the spectrum and variance of the jitter do not require an exact specification of the phase comparator being used as do Saltzberg's and ours but, consequently, they relate the jitter spectrum and variance to more abstract quantities with less physical meaning.

II. GENERAL MODEL

The general PLL model we assume is shown in Fig. 1. The phase $\phi(t)$ of the data signal and the phase $\theta(t)$ of the timing output from the PLL are measured in slots (fractions of a symbol interval) and assumed to be slowly varying in comparison to a symbol interval. The loop is assumed to be in lock.

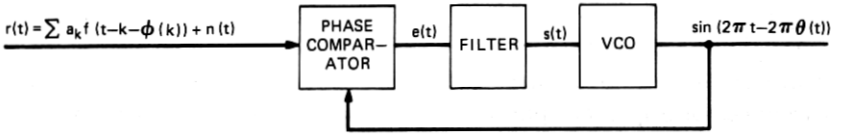

Fig. 1—General model for a PLL timing extractor.

The input data waveform will be taken to have the form*

$$r(t) = \sum a_k f[t - k - \phi(k)] + n(t), \tag{1}$$

where $n(t)$ is additive noise, $f(t)$ is the standard pulse, and the $\{a_k\}$ are the data taking on the values ± 1. The normalization of the symbol interval to unity is without loss of generality and is equivalent to agreeing to measure time (as well as phase) in slots. The assumption of polar (± 1) rather than, say, unipolar (0, 1) signaling is also without loss of generality. The assumption of binary data is restrictive. A generalization of our results for multilevel data would be nontrivial, but should be possible.

Note that, in writing the output of the VCO as $\sin [2\pi t - 2\pi\theta(t)]$, we are not precluding the possibility of the VCO center frequency being offset from the line frequency. With the loop open and a center frequency offset of Δf, the VCO output is expressible as $\sin [2\pi t - 2\pi\theta(t)]$ with

$$\theta(t) = \Delta f t + \theta_0. \tag{2}$$

III. PHASE DETECTORS

To proceed, we need an equation for the error signal $e(t)$ produced by the phase comparator and, thus, we must specify precisely the phase comparator to be considered. In this section, we develop equations for the error signals produced by two different phase comparators: the zero-crossing phase comparator described by Saltzberg[9] and the dead-zone quantizer (DZQ) phase comparator used in the T4M repeater.[11] Characterizing the DZQ phase comparator will allow presenting numerical results.

It happens that the error signal $e(t)$ produced by the DZQ phase comparator is described by equations identical to those describing the error signal produced by the zero-crossing phase comparator if certain constants relating to the pulse shape $f(t)$ and certain random variables relating to the channel noise $n(t)$ are redefined. We expect that the error signals from other phase comparators with transition gating probably also have this same functional form or one very similar to it.

* Summations and integrals written without limits are to be assumed to be from $-\infty$ to $+\infty$.

For this reason, it is felt that, although the analysis of Sections IV through VII is only directly applicable for a zero-crossing phase comparator or a DZQ phase comparator, it can probably be readily extended for any other phase comparator exhibiting transition gating.

3.1 Zero-crossing detector

The zero-crossing phase comparator produces an error signal $e_{ZC}(t)$ that is a train of weighted pulses with separation $T = 1$. The pulse weights are proportional to the time difference between zero crossings of the data waveform and the VCO output. For a PLL with a closed-loop response cutting off well below the symbol rate, as should always be the case, the exact phase of this pulse train and shape of its pulses are unimportant, and we can to good approximation take it to be given by

$$e_{ZC}(t) = \sum e_k \delta(t - k), \tag{3}$$

where $\delta(t)$ is the Dirac delta function and the $\{e_k\}$ are weights.

A typical received data waveform,

$$r(t) = \sum a_k f(t - k - \phi_k) + n(t), \tag{4}$$

where

$$\phi_k \triangleq \phi(k) \tag{5}$$

is drawn in Fig. 2a. It is assumed that $n(t)$ and $\{\phi_k\}$ are identically zero, and that the standard equalized pulse $f(t)$ has a raised cosine shape (see Fig. 2b). Notice that, whenever there is no data transition, there is no zero crossing. In this case, the zero-crossing phase detector sets e_k equal to zero. When the noise $n(t)$ or the input phase samples $\{\phi_k\}$ are not identically zero, or when $f(t)$ is not of its nominal raised-cosine shape, the received waveform is no longer as clean as that shown in Fig. 2a. Nonetheless, it will still maintain the same basic character with zero crossings occurring only with associated data transitions.

Saltzberg cleverly shows in Ref. 9 that, to within excellent approximation, e_k is given by

$$e_k = \alpha_1 d_k(\theta_k - \phi_k - w_k). \tag{6}$$

The proportionality of e_k to the phase error $\theta_k - \phi_k$ through the proportionality constant α_1 is the desired phase comparator response. This desired response is degraded by the on-off gating of the variable

$$d_k = \begin{cases} 1, & a_k \neq a_{k+1} \\ 0, & a_k = a_{k+1} \end{cases} = (1 - a_k a_{k+1})/2 \tag{7}$$

associated with data transitions and the additive disturbance w_k given

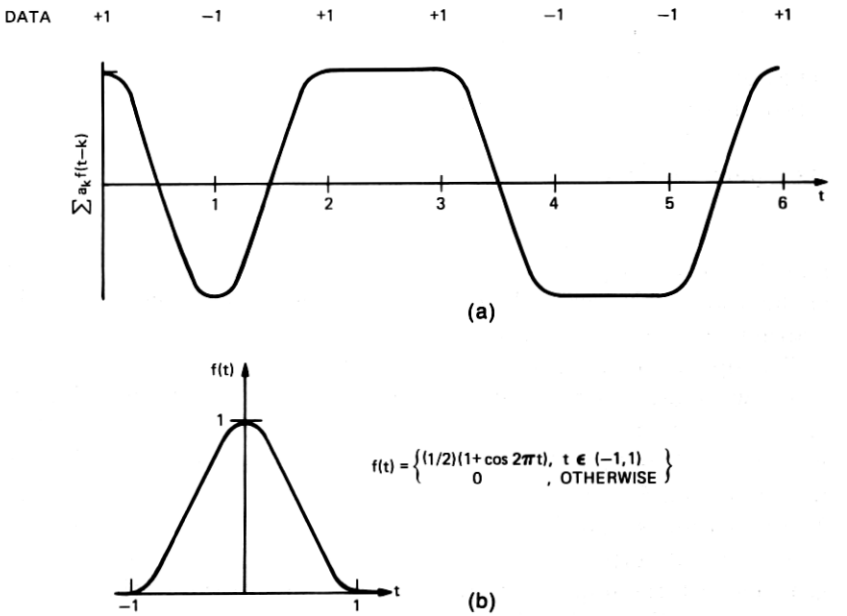

Fig. 2—(a) Nominal received waveform. (b) Raised-cosine pulse.

by

$$w_k = a_k v_k + a_k \sum_m a_{k-m}\epsilon_m, \tag{8}$$

where

$$v_k = \frac{n(k + \frac{1}{2} + \phi_k)}{[\dot{f}(\frac{1}{2}) - \dot{f}(-\frac{1}{2})]} \tag{9}$$

and

$$\epsilon_k = \begin{cases} 0, & k = 0, 1 \\ f(k + \frac{1}{2}), & k \neq 0, 1 \end{cases}. \tag{10}$$

[The pulse $f(t)$ has, without loss of generating, been centered so that $f(\frac{1}{2}) = f(-\frac{1}{2})$]. The two components $a_k v_k$ and $a_k \sum_m a_{k-m}\epsilon_m$ of w_k account for the shift in zero crossings of the received waveform by additive channel noise and by intersymbol interference, respectively. We shall not derive (6) here, since Saltzberg's derivation is quite clear and the derivation of $e_{DZQ}(t)$ in the next section and the appendix, being similar, presents the key ideas.

3.2 DZQ phase detector

The operation of the zero-crossing phase comparator is conceptually simple, but its implementation appears difficult. The dead-zone

quantizer (DZQ) phase comparator, which was first proposed by W. G. Hammett, is more readily implemented and is being used in the T4M repeater. By describing and mathematically characterizing it here, we establish a base for numerical results to be given later.

A block diagram of the DZQ phase comparator is shown in Fig. 3a. Its inputs are the received waveform

$$r(t) = \sum a_k f(t - k - \phi_k) + n(t) \tag{11}$$

and the VCO output $\sin [2\pi t - 2\pi\theta(t)]$. Its only block requiring explanation is the DZQ, which is a memoryless nonlinearity with the transfer function shown in Fig. 3b.

The operation of this phase comparator is illustrated in Fig. 4, where waveforms at the inputs and outputs of all the blocks in Fig. 3a are shown. It is assumed that the data sequence is as indicated, $n(t) = 0$, $\phi(t) = 0$, $f(t)$ has raised cosine shape (nominal for the T4M repeater), and $\theta(t) = \frac{1}{8}$ (that is, the VCO phase is lagging 45 degrees). The true error signal shown on the next-to-last line can be taken, for mathematical purposes, as the train of weighted impulses shown on the last line with the impulse weights equal to the integral of their associated pulses. Notice in Fig. 4 that the phase-comparator output is nonzero only when there is a data transition.

As in the zero-crossing phase comparator, the effect of additive channel noise and intersymbol interference is to make the weights of the impulses in the phase-comparator output differ from strict pro-

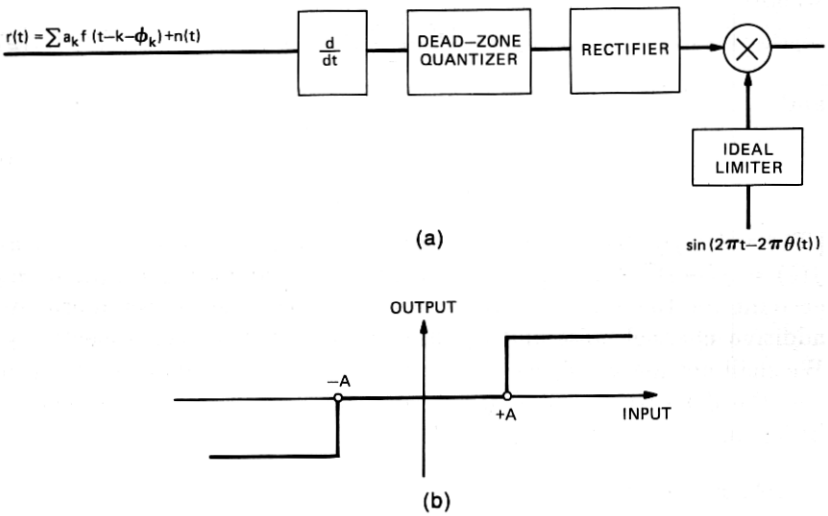

Fig. 3—(a) DZQ phase comparator. (b) Instantaneous transfer function of a dead-zone quantizer.

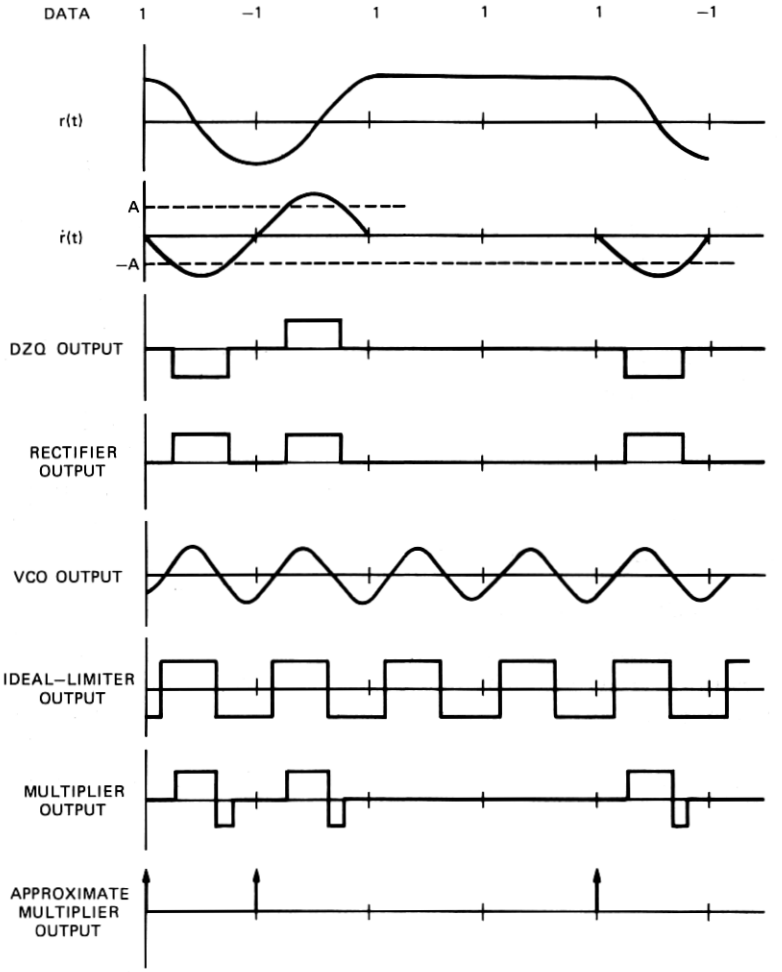

Fig. 4—Waveforms in DZQ phase comparators.

portionality to the difference between $\phi(t)$ and $\theta(t)$ by a small random amount [through $n(t)$ and the data $\{a_k\}$]. Defining the weights of the impulses in the last line of Fig. 4 as $\{e_k\}$, that is, defining

$$e_{DZQ}(t) = \sum e_k \delta(t - k), \tag{12}$$

we show in the appendix that

$$e_k = \alpha_1 d_k(\theta_k - \phi_k - w_k), \tag{13}$$

where all symbols except the channel noise variables $\{v_k\}$ and the intersymbol interference constants $\{\epsilon_k\}$ are as in the discussion of the

zero-crossing phase comparator. The changed definitions are

$$v_k = \frac{\dot{n}(k + \phi_k + \tau^-)}{(2\beta^-)} + \frac{\dot{n}(k + \phi_k + \tau^+)}{(2\beta^+)} \tag{14}$$

and

$$\epsilon_k = \begin{cases} 0, & k = 0, 1 \\ \dot{f}(k + \tau^-)/(2\beta^-) + \dot{f}(k + \tau^+)/(2\beta^+), & k \neq 0, 1 \end{cases}, \tag{15}$$

where

$$\beta^{\pm} = \dot{f}(\tau^{\pm} - 1) - \dot{f}(\tau^{\pm}) \tag{16}$$

and τ^+ and τ^- are defined as in Fig. 5. The pulse $f(t)$ has without loss of generality been centered so that

$$\tau^- + \tau^+ = 1. \tag{17}$$

Thus, the only difference in the two phase comparators is in the precise way in which the random variables $\{v_k\}$ are related to the additive channel noise and the constants $\{\epsilon_k\}$ to the pulse tails.

IV. SWITCHED LINEAR MODEL

Using eqs. (3) and (6) as a characterization of the phase comparator and realizing that the phase of the VCO output is the integral of the signal on its input, we can model the PLL of Fig. 1 as shown in Fig. 6. In Fig. 6, Δf is the difference between the center frequency of the VCO and the line frequency, which we have normalized to unity. The function $H(s)$ is the transfer function of the low-pass filter normalized so that $H(0) = 1$, and the open loop dc gain α is given by

$$\alpha = \alpha_1\alpha_2\alpha_3,$$

where α_1 is the phase-comparator gain [previously defined by eq. (6)], α_2 is the dc gain of the low-pass filter, and α_3 is the VCO gain.

It will be convenient to mix discrete and continuous notation as in Fig. 6. For a precise interpretation of figures such as these, discrete

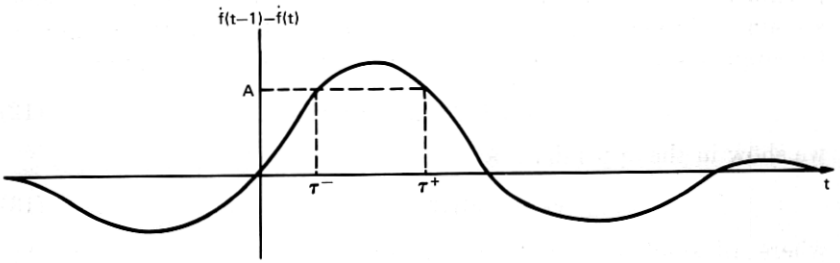

Fig. 5—Defining figure for τ^- and τ^+.

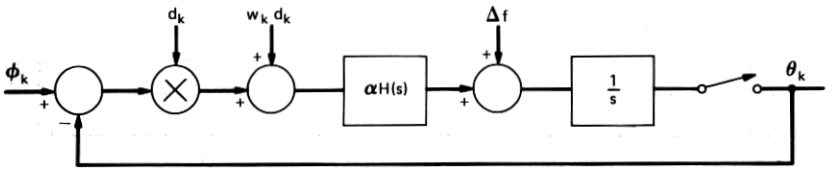

Fig. 6—Time-varying model for PLL.

labels such as θ_k and $w_k + \phi_k$ are to be taken as shorthand for $\sum \theta_k \delta(t - k)$ and $\sum (w_k + \phi_k)\delta(t - k)$.

The model of Fig. 6 is linear, but it varies in time as the gating variable d_k opens and closes the loop. A direct analysis of jitter using this model is made difficult by the gating.

V. TIME-INVARIANT LINEAR MODEL

The key to obtaining a time-invariant approximation is to consider the nature of the signal $(\phi_k - \theta_k)d_k$ at the gate output in Fig. 6. Letting p denote the probability of a data transition, we have

$$(\phi_k - \theta_k)d_k = (\phi_k - \theta_k)p + (\phi_k - \theta_k)(d_k - p). \tag{18}$$

The term $(\phi_k - \theta_k)p$ in this expansion represents the low frequency (in comparison to the symbol rate) response of the gate to the low frequency signal $\phi_k - \theta_k$ on its input. This signal completes the feedback path. Since d_k has mean p and to good approximation is not correlated with $(\phi_k - \theta_k)$, the other component is a wideband signal with no dc. It represents jitter-producing wideband noise injected into the loop by the gating.

Conceptually, the phase error $\phi_k - \theta_k$ has three components: a static offset, which we denote by μ, necessary to pull the VCO from its quiescent frequency to the line frequency; a low-frequency component present when $\phi(t)$ changes faster than the loop can track; and jitter. Our key approximation is

$$(\phi_k - \theta_k)(d_k - p) \doteq \mu(d_k - p). \tag{19}$$

In the PLL timing extractor of the T4M repeater, μ is about 100 times the standard deviation of the jitter when the VCO offset is a worst case 60 parts per million. Also $\phi(t)$, which is typically jitter from previous repeaters, is within the closed-loop bandwidth so that it can be tracked. Thus, for this system approximation (19) is excellent unless the center frequency of the VCO happens to be such that μ is unusually small. In this case, however, approximating the wideband power injected by $(\phi_k - \theta_k)(d_k - p)$ by the wideband power injected by

$$\mu(d_k - p) \doteq 0$$

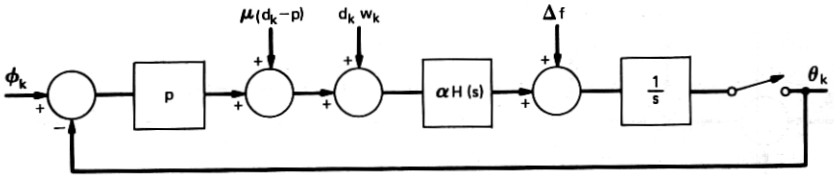

Fig. 7—Approximation to time-varying model.

is still good since the jitter-producing noise injected into the loop by additive channel noise and intersymbol interference is much stronger than that injected by transition gating. We expect that, for most other well-designed phase-locked loops, approximation (19) will be good.

Approximation (19) substituted in (18) gives

$$(\phi_k - \theta_k)d_k \doteq (\phi_k - \theta_k)p + \mu(d_k - p). \tag{20}$$

With this approximation, the model of Fig. 6 becomes the time-invariant model of Fig. 7, which can be further simplified to the model of Fig. 8.

It remains to calculate the static offset μ. Refer to Fig. 6. Since there can be no steady-state dc signal at the integrator input, the dc on the output of the low-pass filter must equal $-\Delta f$, and the dc on its input must equal $-\Delta f/\alpha$. Therefore, with overscores denoting mean values,

$$\overline{(\phi_k - \theta_k)d_k} = -\frac{\Delta f}{\alpha} - \overline{w_k d_k}. \tag{21}$$

We noted earlier that $\phi_k - \theta_k$ and d_k are approximately uncorrelated. Thus,

$$\overline{(\phi_k - \theta_k)d_k} = \overline{(\phi_k - \theta_k)}\,\overline{d_k} = \mu p \tag{22}$$

and

$$\mu = -\frac{\Delta f}{p\alpha} - \frac{\overline{w_k d_k}}{p}. \tag{23}$$

The mean $\overline{w_k d_k}$ is a function of the noise statistics and data statistics. It can be shown that if the data are independent of the noise and have stationary statistics,

$$\overline{w_k d_k} = 0, \tag{24}$$

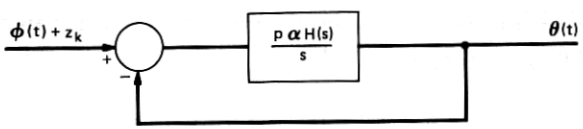

$z_k = (1/p)\,(\omega_k d_k + \mu(d_k - p)) + \Delta f/\alpha$

Fig. 8—Time-invariant linear model for PLL.

in which case

$$\mu = -\frac{\Delta f}{p\alpha}. \tag{25}$$

The model of Fig. 8 gives the output phase $\theta(t)$ as the sum of the input phase $\phi(t)$ passed through a filter with transfer function

$$G(s) = \frac{p\alpha H(s)}{s + p\alpha H(s)} \tag{26}$$

and added noise

$$z_k = \left(\frac{1}{p}\right)\left[w_k d_k + \mu(d_k - p) + \frac{\Delta f}{\alpha}\right] \tag{27}$$

passed through the same filter. Since the model is fixed and linear, it is easily analyzed. Although in the remainder of the paper we concentrate on finding the output-phase spectrum $S_\theta(f)$ for random $\phi(t)$, $n(t)$, and $\{a_k\}$, exact calculations of $\theta(t)$ can be made for given $\phi(t)$, $n(t)$, and $\{a_k\}$.

VI. SPECTRUM AND VARIANCE

The spectrum $S_\theta(f)$ of $\theta(t)$ can be calculated under various assumptions on the statistics of $\phi(t)$, $n(t)$, and the data sequence $\{a_k\}$. We make the calculation here assuming

(*i*) $n(t)$, $\phi(t)$, and the data $\{a_k\}$ are statistically independent and stationary random processes.

(*ii*) The random variables $\{a_k\}$ are independent.

Assumption (*i*) is reasonable if $\phi(t)$ is not to represent accumulated jitter from previous timing extractors.

Let p' denote the probability a data bit equals 1 and let $q' = 1 - p'$. Then

$$p = 2p'q'. \tag{28}$$

Notice that the transition probability is at most $\frac{1}{2}$, which is achieved with equiprobable data.

Assumption (*i*) implies that the driving processes $\phi(t)$ and $\{z_k\}$ in Fig. 8 are independent.* Thus, the spectrum $S_\theta(f)$ of $\theta(t)$ is given by

$$S_\theta(f) = |G(f)|^2 S_\phi(f) + |G(f)|^2 S_z(f), \tag{29}$$

* The $\{z_k\}$ process is a function of the $\{a_k\}$ and $\{v_k\}$ processes. Equation (9) (zero-crossing phase comparator) and eq. (14) (DZQ phase comparator) both give the $\{v_k\}$ process as a function of both the $\phi(t)$ and $n(t)$ processes. Thus, the independence of the $\phi(t)$ and $n(t)$ processes does not at first seem sufficient for the independence of the $\phi(t)$ and $\{v_k\}$ processes. However, the functional forms of both (11) and (18) are such that, in both cases, the univariate statistics of the $\{v_k\}$ process are independent of the statistics of the $\phi(t)$ process [the stationarity of the $n(t)$ process is used here] and moreover to within the slowly-varying $\phi(t)$ assumption already made, the multivariate statistics are also. Thus, the $\phi(t)$ and $\{v_k\}$ processes are independent to excellent approximation.

where $S_\phi(f)$ is the spectrum of $\phi(t)$ and $S_z(f)$ is the spectrum of the process

$$z(t) = \sum_{k=-\infty}^{\infty} z_k \delta(t - k - \lambda), \tag{30}$$

with λ being an epoch-randomizing uniform $[0, 1]$ random variable, the addition of which is necessary to make $z(t)$ stationary. Assuming the loop to be narrowband so that the cutoff of the low-pass function $G(f)$ is well within the band of frequencies over which the spectrum of the wide-band process $z(t)$ is flat, we have, to excellent approximation,

$$S_\theta(f) = |G(f)|^2 S_\phi(f) + |G(f)|^2 S_z(0). \tag{31}$$

Since the variance σ_θ^2 of $\theta(t)$ is the integral of $S_\theta(f)$, we have to this same approximation

$$\sigma_\theta^2 = \int |G(f)|^2 S_\phi(f) df + S_z(0) \int |G(f)|^2 df. \tag{32}$$

The first term of (31) and the first term of (32) are associated with the input phase $\phi(t)$ and will not be considered further. The more interesting second terms are associated with the jitter added by the timing extractor. Notice that $S_z(0)$ provides a measure of the timing extractor's performance.

It can be shown through straightforward but tedious manipulations that

$$S_z(0) = \frac{[C_v(0) - C_v(1)]}{p} + \frac{\mu^2(2 - 3p)}{p} - 2\mu(\epsilon_1 - \epsilon_{-2}) + \sum_{k=1}^{\infty} (\epsilon_k + \epsilon_{-k} - \epsilon_{k-1} - \epsilon_{k-1})^2, \tag{33}$$

where $C_v(k)$ is the covariance function of the sequence $\{v_k\}$. The first term in (33) is associated with additive channel noise and will usually be negligible in comparison to the remaining terms, which are associated with the pulse shape $f(t)$ through the intersymbol-interference constants $\{\epsilon_k\}$ and the vco offset Δf through μ.

It is straightforward to show for either phase comparator that, if $f(t)$ is a symmetric pulse, then

$$\epsilon_k = \epsilon_{-k-1}, \qquad k = 1, 2, \cdots \tag{34}$$

and therefore

$$S_z(0) = [C_v(0) - C_v(1)]/p + \mu^2(2 - 3p)/p. \tag{35}$$

For unknown μ, this is certainly the best that can be done. The design

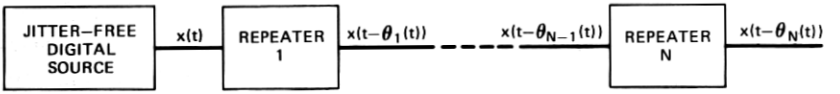

Fig. 9—Jitter accumulation along a chain of repeaters.

conclusion to be drawn from (35) and (31), therefore, is that symmetric pulse shapes are best for timing purposes.

VII. CHAINS

The results of the previous section are easily extended for a cascade of PLL timing extractors. Cascades are of engineering interest for the study of chains of digital repeaters with PLL timing extractors. In a cascade like that of Fig. 9, we call $\theta_N(t)$ *accumulated jitter* and

$$\Delta_N(t) = \theta_N(t) - \theta_{N-1}(t) \tag{36}$$

alignment jitter. The name alignment jitter comes from the fact that $\Delta_N(t)$ represents the amount by which the actual sampling time in the Nth repeater is misaligned from the ideal sampling time.

In Fig. 9, the phase of the output of the $(n-1)$th repeater is the phase of the input to the nth. This fact and the fixed linear model of Fig. 8 imply the model of Fig. 10, where

$$G_n(s) = \frac{p\alpha_n H_n(s)}{s + p\alpha_n H_n(s)}. \tag{37}$$

This general model is fixed and linear, and thus not impossible to analyze by conventional methods for any parameters of interest. However, to derive insight and to obtain reasonably concise expressions for $\theta_N(t)$ and $\Delta_N(t)$, it is necessary to make further assumptions that reduce the number of parameters. We assume

(*i*) The additive channel noise is negligible and therefore the random variables $\{v_k^{(n)}\}$ may be taken as zero.
(*ii*) The equalized pulse shapes $f_n(t)$ at the inputs to all the repeaters are identical.
(*iii*) The VCO offsets Δf_n are all identical.
(*iv*) The filters $H_n(s)$ and open-loop dc gains α_n are all identical.

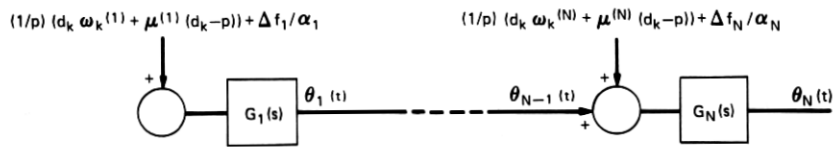

Fig. 10—Model for jitter accumulation along a chain of PLL timing extractors.

Assumption (*i*) is in general reasonable. Assumptions (*ii*) through (*iv*) are less reasonable, but are still interesting in that they are worst-case assumptions. The first two align the input signals in Fig. 10. The last gives the most chain gain at the peak frequency for a specified amount of peaking in each repeater.

With assumptions (*i*) through (*iv*), the model of Fig. 10 simplifies to that of Fig. 11, from which it is apparent that (we are making the wideband noise approximation again)

$$S_{\theta_N}(f) = \left| \sum_{n=1}^{N} G^n(f) \right|^2 S_z(0) \tag{38}$$

and

$$S_{\Delta_N}(f) = |G^n(f)|^2 S_z(0). \tag{39}$$

Interestingly, the model of Fig. 11 is identical to that used by Byrne, Karafin, and Robinson[6] to analyze a chain of digital repeaters with tuned-circuit timing extractors. One important difference, however, between the two analyses is that we have available a formula for $z(t)$ in terms of physically meaningful parameters. Byrne, Karafin, and Robinson did not have such a formula and had to experimentally determine $S_z(0)$.

The variances $\sigma^2_{\Delta_N}$ and $\sigma^2_{\theta_N}$ of $\Delta_N(t)$ and $\theta_N(t)$ are, from (38) and (39), given by

$$\sigma^2_{\Delta_N} = J(N) S_z(0) \tag{40}$$

and

$$\sigma^2_{\theta_N} = I(N) S_z(0), \tag{41}$$

where

$$J(N) = \int |G^N(f)|^2 df \tag{42}$$

and

$$I(N) = \int \left| \sum_{n=1}^{N} G^n(f) \right|^2 df. \tag{43}$$

The large N behavior of $J(N)$ and $I(N)$ depends critically on whether or not $G(f)$ exhibits peaking (i.e., whether or not there exists a frequency f such that $|G(f)| > 1$). When $G(f)$ exhibits peaking, it can be shown by Laplace's method (see, for example, Ref. 12 or

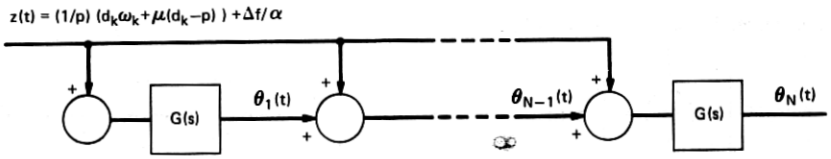

Fig. 11—Simplified model for jitter accumulation along a chain.

Ref. 13) that for large N

$$J(N) \doteq \hat{J}(N) = 2|G(f_p)|^{2N}\sqrt{\pi/[-N\ddot{L}(f_p)]} \tag{44}$$

and

$$I(N) \doteq \hat{I}(N) = \hat{J}(N)\left|\frac{G(f_p)}{1 - G(f_p)}\right|^2, \tag{45}$$

where f_p is the frequency at which $|G(f)|$ is maximum,

$$L(f) = \ln |G(f)|, \tag{46}$$

and $\ddot{L}(f_p)$ is the second derivative of $L(f)$ evaluated at f_p.

When there is no peaking, $G(f)$ is everywhere less than one except at the origin where it must equal one. Thus, as N increases, $|G^N(f)|^2$ and $\sum_{n=1}^{N} |G^n(f)|^2$ become increasingly narrower in bandwidth with amplitudes 1 and N^2 respectively at zero frequency. Let

$$G(f) = \exp\{L(f) + j\phi(f)\} \tag{47}$$

with $L(f)$ and $\phi(f)$ real, and approximate $L(f)$ and $\phi(f)$ near the origin by

$$\begin{aligned} L(f) &\doteq L(0) + \dot{L}(0)f + (\tfrac{1}{2})\ddot{L}(0)f^2 \\ &\doteq (\tfrac{1}{2})\ddot{L}(0)f^2 \end{aligned} \tag{48}$$

and

$$\begin{aligned} \phi(f) &= \phi(0) + \dot{\phi}(0)f \\ &= \dot{\phi}(0)f. \end{aligned} \tag{49}$$

The quantities $L(0)$ and $\dot{L}(0)$ equal zero because $G(f)$ equals one at the origin and $|G(f)|$ is even. The phase $\phi(0)$ equals zero since $G(0)$ is real. Equations (48) and (49) lead after much manipulation to the large N approximations

$$J(N) \doteq \sqrt{\pi/N[-\ddot{L}(0)]} \tag{50}$$

and

$$I(N) \doteq 2\pi N/\dot{\phi}(0). \tag{51}$$

If $G(f)$ is a single-pole characteristic, that is, if

$$G(f) = \frac{1}{1 + jf/f_0}, \tag{52}$$

then (68) reduces to

$$I(N) \doteq 2\pi N f_0, \tag{53}$$

which is consistent with a result in Ref. 6.

Notice the great difference in the asymptotic behavior of $J(N)$ and $I(N)$ in the two situations. With peaking, $J(N)$ and $I(N)$ are asymp-

totically exponential [eqs. (44) and (45)], whereas without peaking $J(N)$ actually decreases with N for large N and $I(N)$ only grows linearly. The rapid growth of (44) and (45) with N indicates that, to control jitter accumulation along a long chain, there must be very little if any peaking.

VIII. NUMERICAL RESULTS

We have used the theory developed here to numerically characterize the jitter performance of the timing extractor in the T4M digital repeater. The exact numbers obtained are, of course, only of direct interest to designers of this repeater, but their relative sizes should be indicative of other timing extractors, and thus of more general interest.

Data on the T4M line are scrambled so that an assumption of independent data is justified, and, furthermore, the probability p of a data transition equals $\frac{1}{2}$. Additive channel noise is a negligible jitter source. The timing loop has a worst-case vco offset of 60 parts per million, a dc gain

$$\alpha = 8 \times 10^{-3}, \tag{54}$$

and a filter

$$H(f) = \frac{(1 + jf/f_1)(1 + jf/f_2)}{(1 + jf/f_3)(1 + jf/f_4)^2(1 + jf/f_5)(1 + jf/f_6)}, \tag{55}$$

where f_1, f_2, f_3, f_4, f_5, and f_6 are, respectively, 3.65×10^{-6}, 3.65×10^{-5}, 1.82×10^{-7}, 7.30×10^{-5}, 1.45×10^{-4}, and 1.09×10^{-3} cycles per slot.*

The reasons for the rather involved form of this filter are of no consequence here. However, it should be pointed out that some of the poles and zeros are fixed by circuit parasitics and are not introduced intentionally.

The shape $f(t)$ of the received and equalized standard pulse depends on repeater spacing and other parameters. A typical waveform $f(t)$ appears in Fig. 12. With a slicing level A fixed at $\frac{3}{4}$ the maximum of $|\dot{f}(t) - f(t-1)|$, the associated intersymbol interference constants $\{\epsilon_k\}$ are as in Table I. Substituting these values and $p = \frac{1}{2}$ in (33) gives

$$S_z(0) = \mu^2 - 2\mu(0.0090) + 1.61 \times 10^{-4}. \tag{56}$$

For $|\Delta f| \leqq 60 \times 10^{-6}$, we have

$$|\mu| = \left|\frac{\Delta f}{p\alpha}\right| \leqq 0.015. \tag{57}$$

* Assuming $T = 1$ is equivalent to measuring time in slots and thus frequency in cycles per slot.

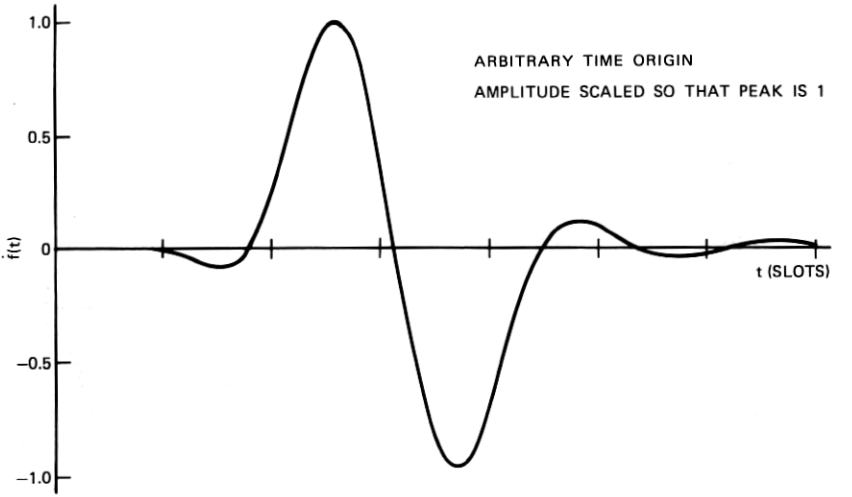

Fig. 12—Output of differentiator.

With $\mu \in [-0.015, 0.015]$,

$$S_z(0) \in [80 \times 10^{-6}, 656 \times 10^{-6}]. \tag{58}$$

The minimum is achieved by

$$\mu = +0.009 \tag{59}$$

and the maximum by

$$\mu = -0.015. \tag{60}$$

All three terms of (33) are of comparable magnitude for these parameters, indicating that for this particular repeater the jitter produced by intersymbol interference is comparable to that produced by transition gating.

Table I — Numerical values for the constants $\{\epsilon_k\}$ having magnitudes greater than 0.00005. The constants ϵ_0 and ϵ_{-1} equal zero by definition

ϵ_{-3}	−0.0009
ϵ_{-2}	0.0194
ϵ_{-1}	0.0000
ϵ_0	0.0000
ϵ_1	0.0284
ϵ_2	−0.0002
ϵ_3	0.0003
ϵ_4	−0.0005
ϵ_5	0.0001

Table II — Integral values and their approximations in dB

N	$\hat{J}(N)$	$J(N)$	$\hat{I}(N)$	$I(N)$
1	−40.0	−38.2	−27.2	−38.2
2	−40.7	−38.9	−28.0	−34.0
3	−40.9	−39.0	−28.1	−31.6
5	−40.6	−38.8	−27.8	−28.6
7	−39.8	−38.3	−27.1	−26.4
10	−38.4	−37.2	−25.7	−23.8
20	−32.7	−32.1	−19.9	−17.2
30	−26.3	−26.0	−13.6	−11.4
50	−12.9	−12.7	−0.2	+0.9
70	0.8	1.0	13.6	14.2
100	21.8	21.9	34.6	35.0
200	92.8	92.9	105.6	105.8
300	164.4	164.5	177.2	177.3
500	308.4	308.4	321.1	321.2

With $p = \frac{1}{2}$, $\alpha = 0.008$, and $H(f)$ as given by (55), $G(f)$ has 0.75 dB of peaking. In Table II we give $\hat{J}(N)$, $J(N)$, $\hat{I}(N)$, $I(N)$, $\sigma^2_{\Delta N}$, and $\sigma^2_{\theta N}$ [as defined by eqs. (44), (42), (45), (43), (40), and (41)] for various values of N. The entries for $\sigma^2_{\Delta N}$ and $\sigma^2_{\theta N}$ assume a worst-case $S_z(0)$ of 6.56×10^{-4}. The convergence of $\hat{J}(N)$ to $J(N)$ and $\hat{I}(N)$ to $I(N)$ for large N is readily apparent. It is also apparent that jitter accumulation limits line lengths on this particular system to about 70 repeaters where the rms alignment jitter is 0.03 slot (10 degrees). The entries in the table for larger N need qualification. One could not expect to measure them since, in that length line, lock would be lost. Our analysis assumes lock and makes many small signal approximations.

IX. CONCLUSIONS

By chopping the phase error $\phi_k - \theta_k$, transition gating injects jitter-producing wideband noise into a PLL extracting symbol timing from a baseband data waveform. If the wideband noise injected by the signal $(\phi_k - \theta_k)(d_k - p)$ is approximated as that injected by $\mu(d_k - p)$, the model for analyzing jitter in a PLL with transition gating becomes time invariant and can be easily analyzed.

X. ACKNOWLEDGMENTS

Ta-Mu Chien first introduced the author to the general problem of characterizing the jitter performance of digital repeaters with PLL timing extractors and, in particular, the theoretical problems associated with transition gating. Much of the timing-extractor circuitry in the T4M repeater was designed by J. A. Bellisio, who provided its characterization data. Throughout our work, M. R. Aaron shared

freely of his insight into this particular problem and his general knowledge of digital transmission.

APPENDIX

Calculation of Error Signal

In this appendix, we find the weights $\{e_k\}$ for the DZQ phase comparator as a function of the input phase, the VCO phase, the data sequence $\{a_k\}$, the standard pulse shape $f(t)$, and the additive channel noise $n(t)$. The procedure followed is quite similar to that used by Saltzberg[9] to find the weights $\{e_k\}$ for the zero-crossing phase comparator.

Assume first, for argument's sake, that $a_k = -1$ and $a_{k+1} = +1$. Then

$$r(t) = -f(t - k - \phi_k) + f(t - k - 1 - \phi_{k+1}) + \sum_{m \neq k, k+1} a_m f(t - m - \phi_m) + n(t). \quad (61)$$

The input jitter ϕ_k contains only low frequencies in comparison to the symbol rate. Thus, the near neighbors of ϕ_k approximately equal it and, assuming $f(t)$ is insignificantly small far out on its tails (as it must be for the eye to be open and regeneration possible), we can reasonably take $r(t)$ for $t \in [k, k + 1]$ as

$$r(t) = -f(t - k - \phi_k) + f(t - k - 1 - \phi_k) + \sum_{m \neq k, k+1} a_m f(t - m - \phi_k) + n(t). \quad (62)$$

Define

$$q(t) = \sum_{m \neq k, k+1} a_m \dot{f}(t - m - \phi_k) + \dot{n}(t). \quad (63)$$

Then

$$\dot{r}(t) = -\dot{f}(t - k - \phi_k) + \dot{f}(t - k - 1 - \phi_k) + q(t). \quad (64)$$

Let τ^- denote the time in $[0, 1]$ when $\dot{f}(t - 1) - \dot{f}(t)$ makes an upward crossing of the DZQ slicing level A and let τ^+ denote the time in $[0, 1]$ when it makes a downward crossing (see Fig. 5). During the time interval $[k + \phi_k, k + 1 + \phi_k]$, $\dot{r}(t)$ will appear as in Fig. 13. Define τ_k^- so that the input to the dead-zone quantizer makes an upward crossing of the slicing level A (that is, a pulse starts at the DZQ output) at time $k + \phi_k + \tau_k^-$. Denote the slope of $\dot{f}(t - 1) - \dot{f}(t)$ at time τ^- by β^-. That is, let

$$\beta^- = \ddot{f}(\tau^- - 1) - \ddot{f}(\tau^-). \quad (65)$$

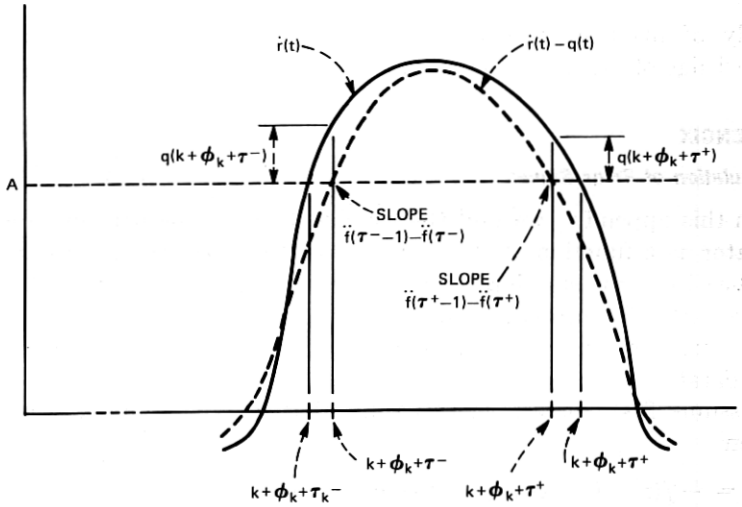

Fig. 13—Linear extrapolation for τ^- and τ^+.

To good approximation, we have (see Fig. 13)

$$\beta^- = \frac{q(k + \phi_k + \tau^-)}{\tau^- - \tau_k^-} \tag{66}$$

or, after rearrangement,

$$\tau_k^- = \tau^- - q(k + \phi_k + \tau^-)/\beta^-. \tag{67}$$

Defining τ_k^+ as the time when the pulse at the output of the dead-zone quantizer ends and defining

$$\beta^+ = \ddot{f}(\tau^+ - 1) - \ddot{f}(\tau^+), \tag{68}$$

we have, by a similar argument,

$$\tau_k^+ = \tau^+ - q(k + \phi_k + \tau^+)/\beta^+. \tag{69}$$

The output of the vco is $\sin [2\pi t - 2\pi\theta(t)]$. Assuming the phase-locked loop is in lock, that is, that $\theta(t) - \phi(t)$ is, at most, a small fraction of a slot, a downward crossing of zero by $\sin [2\pi t - 2\pi\theta(t)]$ must occur near the middle of the interval $[k + \phi_k, k + 1 + \phi_k]$. Define s_k so that

$$k + \phi_k + \tfrac{1}{2} + s_k$$

denotes the time of this occurrence. Then

$$[2\pi(k + \phi_k + \tfrac{1}{2} + s_k) - 2\pi\theta(k + \phi_k + \tfrac{1}{2} + s_k)] \bmod 2\pi = \pi. \tag{70}$$

The phase $\theta(t)$ is slowly varying with respect to the symbol interval.

Therefore,

$$\theta(k + \phi_k + \tfrac{1}{2} + s_k) \doteq \theta(k) = \theta_k. \tag{71}$$

With this approximation, (70) becomes

$$[2\pi(k + \phi_k + \tfrac{1}{2} + s_k) - 2\pi\theta(k)] \bmod 2\pi = \pi, \tag{72}$$

which implies ($\phi_k - \theta_k$ and s_k are small)

$$s_k = \theta_k - \phi_k. \tag{73}$$

From Fig. (14), it is clear that e_k must be proportional to

$$\tfrac{1}{2} + s_k - \tau_k^- - [\tau_k^+ - (\tfrac{1}{2} + s_k)], \tag{74}$$

which simplifies to

$$1 + 2s_k - \tau_k^- - \tau_k^+ \tag{75}$$

or, after substituting (74) for s_k,

$$2(\theta_k - \theta_k) + 1 - \tau_k^- - \tau_k^+. \tag{76}$$

Using the approximations (67) and (69) for τ_k^- and τ_k^+ and denoting the constant of proportionality relating e_k and (76) by $\alpha_1/2$, we have

$$e_k = \alpha_1(\theta_k - \phi_k) + \alpha_1(1 - \tau^- - \tau^+)/2 + \alpha_1\left\{\frac{q(k + \phi_k + \tau^-)}{2\beta^-} + \frac{q(k + \phi_k + \tau^+)}{2\beta^+}\right\}. \tag{77}$$

Let

$$v_k = \frac{\dot{v}(k + \phi_k + \tau^-)}{2\beta^-} + \frac{\dot{v}(k + \phi_k + \tau^+)}{2\beta^+} \tag{78}$$

and

$$\epsilon_k = \frac{\dot{f}(k + \tau^-)}{2\beta^-} + \frac{f(k + \tau^+)}{2\beta^+} \tag{79}$$

and assume that the pulse $f(t)$ has without loss of generality been centered so that

$$\tau^- + \tau^+ = 1. \tag{80}$$

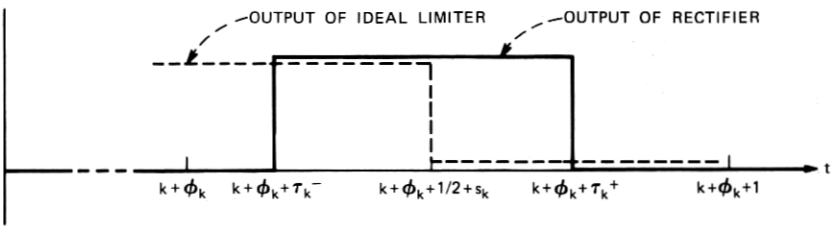

Fig. 14—Inputs to multiplier.

Then, using (63), we obtain

$$e_k = \alpha_1(\theta_k - \phi_k + v_k + \sum_{m \neq k, k+1} a_m \epsilon_{k-m}). \tag{81}$$

To derive (81), we assumed a_k equal to -1 and a_{k+1} equal to $+1$. If the signs are reversed, a similar analysis shows

$$e_k = \alpha_1(\theta_k - \phi_k - v_k - \sum_{m \neq k, k+1} a_m \epsilon_{k-m}). \tag{82}$$

If $a_k = a_{k+1}$,

$$e_k = 0, \tag{83}$$

since no transition occurs. By defining

$$d_k = \begin{Bmatrix} 1, & a_k \neq a_{k+1} \\ 0, & a_k = a_{k+1} \end{Bmatrix} = \frac{(1 - a_k a_{k+1})}{2}, \tag{84}$$

we can combine all three of these equations, and write for all a_k, a_{k+1}

$$e_k = \alpha_1 d_k(\theta_k - \phi_k - a_k v_k - a_k \sum_{m \neq k, k+1} a_m \epsilon_{k-m}). \tag{85}$$

REFERENCES

1. M. R. Aaron, "PCM Transmission in the Exchange Plant," B.S.T.J., *41*, No. 1 (January 1962), pp. 99–141.
2. E. D. Sunde, "Self-Timing Regenerative Repeaters," B.S.T.J., *36*, No. 4 (July 1957), pp. 891–938.
3. W. R. Bennett, "Statistics of Regenerative Digital Transmission," B.S.T.J., *37*, No. 6 (November 1958), pp. 1501–1542.
4. H. E. Rowe, "Timing in a Long Chain of Regenerative Binary Repeaters," B.S.T.J., *37*, No. 6 (November 1958), pp. 1543–1598.
5. M. R. Aaron and J. R. Gray, "Probability Distribution for the Phase Jitter in Self-Timed Reconstructive Repeaters for PCM," B.S.T.J., *41*, No. 2 (March 1962), pp. 503–558.
6. C. J. Byrne, B. J. Karafin, and D. B. Robinson, "Systematic Jitter in a Chain of Digital Regenerators," B.S.T.J., *42*, No. 6 (November 1963), pp. 2679–2714.
7. J. M. Manley, "The Generation and Accumulation of Timing Noise in PCM Systems—An Experimental and Theoretical Study," B.S.T.J., *48*, No. 3 (March 1969), pp. 541–613.
8. T. Takaci, T. Saito, and K. Mano, "Evaluation of Phase Jitter in a Limiter-Tuned Circuit PCM Self-Timing System in Band-Limited Baseband Gaussian Channel," Report of the Research Institute of Electrical Communication, Tohoku University, *22*, 1971, pp. 41–55.
9. B. R. Saltzberg, "Timing Recovery for Synchronous Binary Data Transmission," B.S.T.J., *46*, No. 3 (March 1967), pp. 593–622.
10. E. Roza, "Analysis of Phase-Locked Timing Extraction Circuits for Pulse Code Transmission," IEEE Trans. on Communications, *COM-22*, September 1974, pp. 1236–1249.
11. F. D. Waldhauer, "A Two-Level 274 Mb/s Regenerative Repeater for T4M," Proceedings of the 1975 International Conference on Communications, June 1975.
12. A. Papoulis, *The Fourier Integral and Its Applications*, New York: McGraw-Hill, 1962.
13. J. T. Harvey and J. W. Rice, "Random Timing Noise Growth in a Cascaded Digital Regenerator Chain," IEEE Trans. on Communications, *COM-21*, August 1973, pp. 969–971.